



A fuzzy clustering based segmentation system as support to diagnosis in medical imaging

Francesco Masulli ^{a,*}, Andrea Schenone ^b

^a *Istituto Nazionale per la Fisica della Materia and Dipartimento di Informatica e Scienze dell'Informazione, Università di Genova-Via Dodecaneso 35, 16146, Genova, Italy*

^b *Istituto Nazionale per la Ricerca sul Cancro, Largo R. Benzi 10, 16132, Genova, Italy*

Received 15 January 1998; received in revised form 20 July 1998; accepted 16 October 1998

Abstract

In medical imaging uncertainty is widely present in data, because of the noise in acquisition and of the partial volume effects originating from the low resolution of sensors. In particular, borders between tissues are not exactly defined and memberships in the boundary regions are intrinsically fuzzy. Therefore, computer assisted unsupervised fuzzy clustering methods turn out to be particularly suitable for handling a decision making process concerning segmentation of multimodal medical images. By using the possibilistic c-means algorithm as a refinement of a neural network based clustering algorithm named capture effect neural network, we developed the possibilistic neuro fuzzy c-means algorithm (PNFCM). In this paper the PNFCM has been applied to two different multimodal data sets and the results have been compared to those obtained by using the classical fuzzy c-means algorithm. Furthermore, a discussion is presented about the role of fuzzy clustering as a support to diagnosis in medical imaging. © 1999 Elsevier Science B.V. All rights reserved.

Keywords: Fuzzy diagnosis; Multimodal medical images; Possibilistic neuro fuzzy c-means algorithm; Segmentation

* Corresponding author. Tel.: +39-010-3536297; fax: +39-010-311066.

E-mail address: masulli@disi.unige.it (F. Masulli)

1. Introduction

In clinical field, the fuzzy diagnosis concept is widely applied. It can range between the supervised classification of a number of clinical cases within different classes of pathologies, through a set of rules concerning both linguistic and numerical data, and the unsupervised segmentation of medical images, through data based methods of analysis concerning spatially distributed numerical variables. In all these cases large uncertainty is present in data as well as in rules and this suggests that fuzzy methods can be successfully applied thanks to their intrinsic flexibility. In this paper we focus our attention on methods for the segmentation of multimodal medical images.

Today, medical images are obtained by different acquisition modalities, including X-ray tomography (CT), magnetic resonance imaging (MRI), single photon emission tomography (SPECT), positron emission tomography (PET), ultrasounds (US), etc. [14].

Multimodal volumes can be derived from a set of such different diagnostic volumes carrying complementary information (e.g. both structural and functional) provided by medical imaging technology. An efficient analysis of multimodal medical imaging volumes is an inherently complex task where each component of the data structure, that is, the spatial distribution of the values of a single feature, must be considered together with all the other components. For these reasons, the visual inspection of a large set of such volumetric images permits the physician to only partially exploit the whole global information.

Computer-assisted approaches may be particularly helpful in the clinical oncological field as a support to diagnosis, in order to delineate volumes that have to be treated with radiotherapy and surgery, and to assess quantitatively (in terms of tumor mass or detection of metastases) the effect of oncological treatments. The extraction of such volumes, or other entities of interest, from imaging data is called segmentation and it is usually performed, in the image space, defining sets of voxels with similar features within a whole multimodal volume. The *segmentation* can be described as the definition of clusters, in the multimodal feature space, whose points are associated to similar sets of intensity values in the different images. As a consequence, in this approach the *clustering* process is the main step in the segmentation procedure [5,20,15,21,10], and clustering-based techniques have been shown to be more robust to noise in discrimination of different tissues than techniques based on edge detection [5].

Moreover, volumes of interest in medical imaging are not strictly bounded and the application of segmentation methods to multimodal data is difficult and often a lot expensive in terms of time because of complex geometries.

Supervised methods have been largely employed in medical imaging segmentation studies but they require conditions difficult to satisfy in the clinical field. First of all, they require the labeling of a set of prototypical samples in order to apply the process of generalization. Even if the number of clusters is predefined, a careful labeling of voxels in the training set, belonging with certainty to the different clusters, is not trivial, especially when it concerns multimodal data sets. Moreover,

users have to introduce bias in consequence of the large inter-user variability, generally observed when manual labeling is performed. On the contrary, unsupervised approaches self-organize the implicit structure of data and make clustering of the feature space with no need any user's definition of training regions [3,8] and, finally, the multidimensionality of data is better exploited.

Some considerations about the possible solutions seem adequate. Physicians are hardly able, at least for low level steps in image analysis, to describe the rationale of their decisions. For higher levels, although rationales are more clearly defined, they strongly depend on the different clinical frameworks, on the different anatomical areas, on the different theoretical approaches, etc. As a consequence, it is often impossible to establish well-grounded rule based systems, and data driven approaches have been preferred in most cases.

In such data driven systems, on one hand, a supervised approach has two major drawbacks: is very time-consuming (especially for large volumes) and heavy biases may be introduced by unskilled or fatigued physicians. On the other hand, in clinical practice there is a strong demand for physicians who control both the sequence of choices and of results of the analysis process in order to introduce their theoretical and heuristic knowledge.

Moreover, uncertainty is largely present in medical images, because of the noise in acquisition and of the partial volume effects. This means that voxel values, especially at the borders between volumes of interest, correspond to mixtures of different anatomical tissues, because of the low resolution of sensors. As a consequence, borders between tissues are not exactly defined and memberships in boundary regions are intrinsically fuzzy.

From all these considerations our choice has been a data driven system, whose computational core is grounded on fuzzy clustering, mostly unsupervised but with powerful interactive tools for knowledge based refinements.

In the next section, the problem of segmentation of multimodal images through clustering is discussed. In Sections 3 and 4 we describe the neuro-fuzzy clustering algorithm used. In Section 5, the obtained results are shown and discussed. Conclusions concerning fuzzy algorithms as support to diagnosis are presented in Section 6.

2. From clustering to segmentation

Let us consider a multimodal volume resulting from the spatial registration of a set of s different imaging volumes. Its voxels are associated with an array of s values, each representing the intensity of a single imaging volume in a voxel. In other words, the s different intensity values related to all the voxels in such multimodal volumes can be viewed as the coordinates of the voxels within an s -dimensional feature space where multimodal analysis can be made.

Two different spaces have therefore to be considered for a more complete description of the segmentation problem:

- an image space (usually 3D) defined from the spatial coordinates of the data set, and;
- a multidimensional feature space, as described before.

The interplay between these two spaces turns out to be very important in the task of understanding the data structure. Actually, the definition of clusters, within the above described s -dimensional feature space, and the classification of all the voxels of the volumes to the resulting classes, are the main steps in segmenting multimodal volumes.

In a previous paper [20], we described an interactive system based on a X-Windows Motif interface supporting a full sequence of analysis of multimodal medical images. The functions performed by this system are: feature extraction, dimensionality reduction, unsupervised clustering, voxel classification and intra- and post-processing refinements. As pointed out above, the main element of the whole segmentation system is the unsupervised clustering algorithm used within the segmentation sequence.

In order to improve the efficiency of this task, we have studied different clustering algorithms. Besides the classic c -means (CM) algorithm [6] and a neural network based algorithm, called capture effect neural network (CENN) [7], we made several experiments with a number of fuzzy approaches to clustering for medical image segmentation. These methods seem to adaptively perform an efficient unsupervised clustering, not affected by the dimensionality of the feature space. Moreover, fuzzy clustering methods produce a voxel classification, related to the membership function of clusters, and can add some kind of smoothness to voxel classification. This helps to better define surfaces of the anatomical objects described by segmentation.

The first fuzzy method we studied is the fuzzy c -means (FCM) algorithm by J. Bezdek [4]. The FCM algorithm needs an a priori definition of the number of classes and its results critically depend on this choice. The application of this algorithm to the segmentation of multimodal medical imaging has been described in [15].

The second one is the maximum entropy principle [9] based fuzzy clustering (MEP-FC) method [18,19,2]. It avoids any a priori assumption on the number of classes. Methodology and results of the implementation of this algorithm, concerning the segmentation of multimodal medical imaging, have been shown in previous papers [16,15].

At last, we made experiments with the two versions of the possibilistic c -means (PCM) algorithm [12,13] that, as shown in the next Section 3, relax the probabilistic constraint of the previous methods and give absolute values of membership, or *typicality*, for points in a *fuzzy* set (or cluster). Moreover, starting from an oversized number of clusters, the PCM algorithm, like MEP-FC algorithm, can find the *natural* number of clusters in a data set.

In our experiments, the second version of the possibilistic c -means (PCM-II) algorithm [13], used as a refinement step of the results of CENN, has produced the best results in segmentation. As a consequence, with the addition of a heuristic final step designed to merge redundant clusters, a possibilistic PNFCM algorithm has been defined. It has turned out to be the most suitable for our goals.

In the next sections, the PNFCM algorithm is described and results are presented for two clinical data sets.

3. The possibilistic c-means algorithm

The possibilistic approach to clustering by Keller and Krishnapuram [12,13] assumes that the membership function of a point in a *fuzzy* set (or cluster) is absolute, i.e. it is an evaluation of a *degree of typicality* not depending on the membership values of the same point in other clusters. By contrast, many clustering approaches (such as CM [6], FCM [4] and MEP-FC [18,2]) impose a *probabilistic constraint*, according to which the sum of the membership values of a point in all the clusters must be equal to one.

In [12,13], Krishnapuram and Keller present two version of a possibilistic c-means algorithm (PCM) that relax the probabilistic constraint, in order to allow a possibilistic interpretation of the membership function as a *degree of typicality*.

Let $X = \{\mathbf{x}_k | k = 1, \dots, n\}$ be the set of unlabeled samples; $Y = \{\mathbf{y}_j | j = 1, \dots, c\}$ be the set of cluster centers (or prototypes); and $U = [u_{jk}]$ be the *fuzzy membership matrix*. In the PCM, the elements of U fulfill the following conditions:

$$u_{jk} \in [0, 1] \quad \forall j, k; \quad (1)$$

$$0 < \sum_{k=1}^n u_{jk} < n \quad \forall j; \quad (2)$$

$$\bigvee_j u_{jk} > 0 \quad \forall k. \quad (3)$$

The first possibilistic c-means algorithm (PCM-I) proposed by Krishnapuram and Keller [12] is based on a modification of the objective function of FCM [4]. In this case, one must supply the values of parameters such as the *fuzzifier parameter*, and of those regulating the spread of membership functions [12,1].

PCM-II [13] is based on a modification of the CM [6] (instead of the FCM) cost function in order to avoid the determination of the fuzzifier parameter. The objective function of the PCM-II contains two terms, the first one is the objective function of the CM [6], while the second is a regularizing term. Thanks to this regularizing term, points with a high degree of typicality have high u_{jk} values, and points not very representative have low u_{jk} values in all the clusters:

$$J_m(U, \mathbf{Y}) = \sum_{j=1}^c \sum_{k=1}^n u_{jk} E_j(\mathbf{x}_k) + \sum_{j=1}^c \#_j \sum_{k=1}^n (u_{jk} \log u_{jk} - u_{jk}), \quad (4)$$

where $E_j(\mathbf{x}_k) = \|\mathbf{x}_k - \mathbf{y}_j\|^2$ is the squared Euclidean distance, and the parameter g_j depends on the distribution of points in the j th cluster, and must be assigned before the clustering procedure.

Note that if the second term of $J_m(U, \mathbf{Y})$ is omitted, the elimination of the probabilistic constraint leads to a trivial solution of the minimization of the remaining cost function, that is $u_{jk} = 0 \quad \forall j, k$.

If one searches for clusters with similar distribution, ϱ_j could be set to the same value for each cluster. In general, it is assumed that ϱ_j depends on the average size and on the shape of the j th cluster.

As demonstrated by Krishnapuram and Keller [13], the pair (U, Y) minimizes J_m , under the constraints (1–3) only if:

$$u_{jk} = \exp \left\{ \frac{E_j(\mathbf{x}_k)}{\#_j} \right\} \quad \forall j, k, \quad (5)$$

and

$$y_j = \frac{\sum_{k=1}^n \mathbf{x}_k u_{jk}}{\sum_{k=1}^n u_{jk}} \quad \forall j. \quad (6)$$

This theorem provides the conditions for minimizing the cost function $J_m(U, Y)$. Eqs. (5) and (6) can be interpreted as formulas for recalculating the membership functions and the cluster centers. If we start with an over-dimensioned number of clusters c , redundant centers move to very close positions, and the natural number of clusters can be found by merging clusters with quasi-coincident centers.

A bootstrap clustering algorithm has to be executed before starting PCM, in order to obtain an initial distribution of prototypes in the feature space and to estimate some parameters used in the algorithm. By considering an FCM bootstrap for the PCM [12,13], the following definition of ϱ_j is initially used:

$$\#_j \equiv \frac{\sum_{k=1}^n (u_{jk})^m E_j(\mathbf{x}_k)}{\sum_{k=1}^n (u_{jk})^m}, \quad (7)$$

where $m \in (1, +\infty)$ is the fuzzifier parameter used by the FCM and K is a normalization parameter. This definition makes ϱ_j proportional to the mean value of the intracluster distance and critically depends on the choice of K (in [12] it has been suggested $K = 1$).

In a following optional refinement step a second definition of ϱ_j is used:

$$\#_j \equiv \frac{\sum_{\mathbf{x} \in (\pi_j)_\alpha} E_j(\mathbf{x}_k)}{|(\Pi_j)_\alpha|}, \quad (8)$$

where $(\Pi_j)_\alpha$ is the set of points of the j th cluster whose membership function is over a given threshold α (α -cut). This definition is a less noise sensitive evaluation of the mean value of the intracluster distance obtained by using only points belonging to an α -cut.

The PCM-II starts from the solutions of the bootstrap clustering algorithm and is based on two Lloyd–Picard iterations, the first one using Eq. (7), and the second one using Eq. (8) [12], as shown in Fig. 1.

The use of FCM as a bootstrap for the PCM, involves the problem of the estimation of the fuzzifier parameter m and of the number of clusters c . Sometimes, even if c has been over-dimensioned, FCM aggregates close clusters, characterized by large scatter of points, in one unique cluster. This gives rise to a bias if the FCM is used as a bootstrap for the PCM. Moreover, intracluster distances, obtained by an algorithm with a probabilistic constraint, are used to calculate membership parameters for a possibilistic algorithm: this often produces a misdefinition of the Q_j .

Possibilistic Fuzzy C-Means (PCM-II) algorithm

- Bootstrap Clustering Technique

- train the FCM with a large c and obtain \mathbf{y}_j^0 ;
- compute $U^{(0)}$ using Eq. 5 and Q_j using Eq. 7;
- set the iteration counter l to 0 and initialize the stop parameter ϵ ;

- Basic Iteration

Repeat

- update the prototypes using Eq. 6;
- compute $U^{(l+1)}$ using Eq. 5;
- increment l ;

Until

$$\bigvee_k \|\mathbf{y}_k^{l+1} - \mathbf{y}_k^l\| \leq \epsilon ;$$

Optional Refinement

- reestimate Q_j using Eq. 8;

- Repeat

- update the prototypes using Eq. 6;
- compute $U^{(l+1)}$ using Eq.5;
- increment l ;

Until

$$\bigvee_k \|\mathbf{y}_k^{l+1} - \mathbf{y}_k^l\| \leq \epsilon .$$

Fig. 1. Possibilistic fuzzy c-means (PCM-II) algorithm.

For these reasons we propose, in this paper, the PNFCM, a new neuro-fuzzy version of the PCM-II which uses, as bootstrap, the CENN [7] algorithm. CENN automatically obtains a robust estimation of the number c of *natural* clusters, and of their centers and radii. In particular, the estimation of radii is a very helpful information that is closely related with the intracluster distance.

In the Section 4 we describe the CENN algorithm and in Section 5 we shall present the PNFCM algorithm.

4. The capture effect neural network

The CENN [7] is a self-organizing neural network able to take into account the local characteristics of the point-distribution (*adaptive resolution clustering*). CENN combines standard competitive self-organization of the weight-vectors [11] with a non-linear mechanism of adaptive local modulation of receptive fields (RFs) of neurons (*capture effect*). The **learning phase** of CENN consists of the training step, performing a vector quantization of data, and the labeling step, where the prototypes, obtained by performing the previous step, are grouped in order to obtain robust clusters.

In the **training step** an initial great deal of neurons $n_i = \{\mathbf{w}_i, r_i\}$ is assumed and initialized with randomly chosen weight vectors \mathbf{w}_i (representing centers of sub-clusters), and with large radii $r_i (r_i = R_0)$ of the receptive fields RF_i (modeled by Gaussian functions γ)¹. After that, the data set is presented to CENN and the following learning formulas are applied:

$$\Delta w_i = \eta_w (\mathbf{x}_k - \mathbf{w}_i) \frac{\gamma(d_j(\mathbf{x}_k))}{\sum_l \gamma(d_l(\mathbf{x}_k))} \quad (9)$$

$$\Delta r_i = \begin{cases} \eta_r & (d_i(\mathbf{x}_k) - r_i) \exp(-d_i(\mathbf{x}_k)/p) \\ 0 & \text{if } d_i(\mathbf{x}_k) \geq R_0 \end{cases} \quad (10)$$

where η_w and η_r are learning rates, $d_i(\mathbf{x}_k) = \|\mathbf{x}_k - \mathbf{w}_i\|$ is the Euclidean distance of points to weight vectors, and the parameter p is defined as:

$$p \equiv \frac{\langle d_i(\mathbf{x}_k) \rangle}{D \ln 10}, \quad (11)$$

assuming D as the dimension of the feature space.

The **labeling step** discards any neuron n_q with $r_q = R_0$ (i.e. neurons not representing elements of the training set) and then pairs of neurons, n_p and n_q , will receive the same label (i.e. their associated clusters are merged) if

$$\|\mathbf{w}_p - \mathbf{w}_q\| < (r_p + r_q)\sigma, \quad \sigma \in (0, 1), \quad (12)$$

¹ The radius of a Gaussian RF is defined as the radius of an α -cut of RF itself.

i.e., if they have (partially) overlapped RFs. The parameter σ is called the *degree of overlapping*. This process obtains c groups of neurons \mathcal{G}_j , $j = 1, \dots, c$. We can then define the center and radius of a cluster, related to the j th group, as:

$$\mathbf{y}_j \equiv \langle \mathbf{w} \cdot \rangle_{\mathcal{G}_j} \quad r_j \equiv \langle r \cdot \rangle_{\mathcal{G}_j}. \quad (13)$$

A remaining isolated neuron n_q is called *associable* to a group \mathcal{G}_j ; if

$$\|\mathbf{w}_p - \mathbf{w} \cdot\| < (r_p + r \cdot) \quad (14)$$

at least for one neuron $n \cdot$ of group \mathcal{G}_j .

For such neurons associable to one or more groups, the following completion rule of the labeling step is applied: an isolated neuron n_q , associable to different groups, is assigned to the i th group if and only if

$$i = \arg \min_j (r_{\mathcal{G}_j} - r_q) \quad \forall j. \quad (15)$$

In the **operative phase** an unknown vector \mathbf{x} will be classified by exploiting the winner-take-all (WTA) rule in the following way:

$$\mathbf{x} \in (j\text{th cluster}) \Leftrightarrow h = \arg \min_i \frac{\|\mathbf{x} - \mathbf{w}_i\|}{r_i}, \quad \mathbf{w}_i \in \mathcal{G}_j. \quad (16)$$

After the learning phase:

- the distribution of the prototypes in the feature space approaches the optimal vector quantization scheme of the input data distribution, i.e., it approximates the mixture probability density function;
- the radial size of the RF of each neuron reaches a stable value which is closely related to the spatial density of input data locally around the weight-vector (that is the center of the RF).

5. The possibilistic neuro-fuzzy c-means algorithm

In testing CENN as unsupervised clustering algorithm for the segmentation of multimodal medical images [20], we found some limits and merits of this type of neural network.

The principal limits of the CENN are, mainly, the difficulty in obtaining good results for the problems with high dimensionality and a non-negligible variability of results for classes poorly represented in the data distribution. On the contrary, especially when the feature space has few dimensions, the main advantages of CENNs are the speed and the reliability, i.e. the probability to obtain a nearly correct solution to the clustering problem.

Moreover, the CENN shows some relevant characteristics, such as the capability to automatically produce a robust estimation of the number of natural clusters c , and of their centers \mathbf{y}_j and radii r_j , related with q_j (i.e., $q_j = f(r_j)$).

These characteristics make the CENN a very useful method. In fact, it can act as a robust and unbiased bootstrap procedure for the PCM, overcoming, the limits of FCM, pointed out in Section 3. As shown in Fig. 2, the PNFPCM, uses the CENN

Possibilistic Neuro-Fuzzy C-Means (PNFCM) algorithm

- CENN Bootstrap

- train and label the Capture Effect Neural Network and obtain c , \mathbf{y}_j^0 , and ϱ_j ;
- compute $U^{(0)}$ using Eq. 5;
- set the iteration counter l to 0 and initialize the stop parameter ϵ ;

- PCM-II Basic Iteration

Repeat

- update the prototypes $\mathbf{y}_j^{(l+1)}$ using Eq. 6;
- compute $U^{(l+1)}$ using Eq. 5;
- increment l ;

Until

$$\bigvee_j \|\mathbf{y}_j^{l+1} - \mathbf{y}_j^l\| \leq \epsilon ;$$

- Merging redundant clusters

- group clusters with weighted distance (defined in Eq. 17) less than 10ϵ .

Fig. 2. Possibilistic neuro-fuzzy c-means (PNFCM) algorithm.

as bootstrap for the basic iteration of the PCM-II, and then applies a merging step joining clusters with centers in very close positions with respect to a weighted distance defined as:

$$\tau_{ij} \equiv \frac{\|\mathbf{y}_i - \mathbf{y}_j\|}{\#_i + \#_j}. \quad (17)$$

Note that the refinement procedure of PCM-II (see Fig. 1) is not still necessary.

It is worth to point out that in the PNFCM algorithm the number of clusters c is not imposed at the initialization, but is automatically found by the algorithm itself. In our application, the number of clusters varies from patient to patient even for the same anatomical region (and even from slice to slice), because of the different configurations of the anatomical structures, and of the presence of tumors masses or anatomical anomalies. Besides the better results obtained (as shown in the next section), this is the general motivation of PNFCM, together with the interpretation of memberships values as degrees of typicality.

In different applications, where the number of classes is already known, one can fruitfully apply other improvements to the possibilistic c-means, such as the mixed model proposed by Pal et al. [17].

6. Results and discussion

We have implemented the PNFCM algorithm as a clustering module of our graphical interactive system supporting the full sequence of multimodal medical volumes analysis. In this section we discuss its application to two different multimodal data sets. Both data sets are multimodal volumes composed by three different MRI volumes (T1-weighted, T2-weighted, proton density).

The first data set is from the head of a normal individual and the task is to discriminate white and grey matter, cerebro-spinal fluid, eyes and other structures of interest in order to point out morphological abnormalities.

The second data set is from the head of an individual with meningioma and the task is to define the contours of the tumor located in the right frontal lobe, in order to correctly separate the tumor from a large amount of edema, and to define, where it is possible, the borders of the brain structures in order to formulate a correct differential diagnosis.

In both cases the fusion of the volumes produces a three-modal data set. Each triplet of voxel intensity in the multimodal data set is represented by a point in a 3D feature space whose coordinates represent the intensity values, in that voxel, of each volume belonging to the multimodal data set.

Let us compare the results produced by the different clustering algorithms on transversal slices of the two multimodal volumes. Since our goal was to compare the different unsupervised segmentation algorithms and not to test the overall performances of the interactive segmentation system, the images have been analyzed as they were, without using preprocessing operations like thresholding, contrast enhancement, dimensionality reduction by principal component analysis, and definition of regions of interest. Moreover, results are presented without post processing improvements through morphological operators, or other tools.

For the normal individual, the original images are 171×220 with 256 grey levels and are shown in Fig. 3. The unsupervised segmentation with CENN is shown in Fig. 4a. The CENN algorithm autonomously found five classes with general good performances but with a clear overestimation for the white matter.

In comparison with the FCM algorithm², trained with the same number of classes (Fig. 4b), a large misclassification in the skull is present and thin structures near the eyes result poorly defined while a better definition of the white/grey matter in the brain is shown.

The PNFCM algorithm³ keeps in general the good findings of the CENN bootstrap concerning non-brain structures, improving, moreover, its performances in order to obtain a classification, of white matter and grey matter, better than FCM's (Fig. 4c).

² In our experiments with the FCM we took the localization error of cluster centers as $\epsilon = 2.5$, and $m = 2$, while the centroids were initialized at random.

³ In our experiments with the PNFCM we took the localization error of cluster centers as $\epsilon = 2.5$, and a good evaluation for the PCM-II step of the intracluster distance turned out to be $\varrho_j = \sqrt[D]{r_j}$, where D is the dimensionality of the feature space and r_j is obtained by the CENN bootstrap.

For the individual with meningioma the original images are 256×256 with 256 grey levels and are shown in Fig. 5. In Fig. 6a the results of the unsupervised segmentation with CENN are shown. The CENN algorithm has autonomously

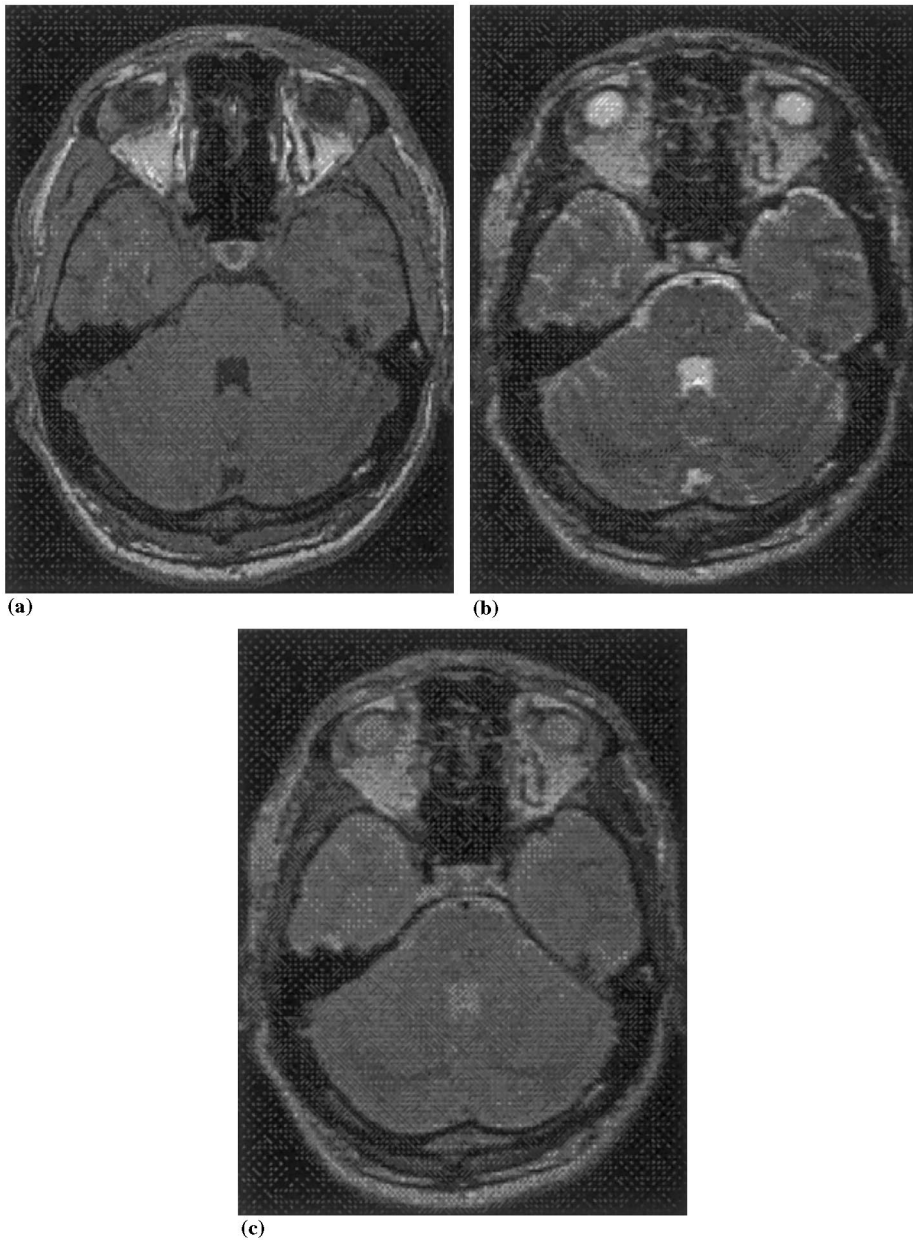


Fig. 3. T1-weighted (a), T2-weighted (b), and proton density (c) MRI images of a normal patient.

found ten classes with some redundancy. If we start the FCM algorithm with the same number of classes, the results (Fig. 6b) may be compared with the CENN ones.

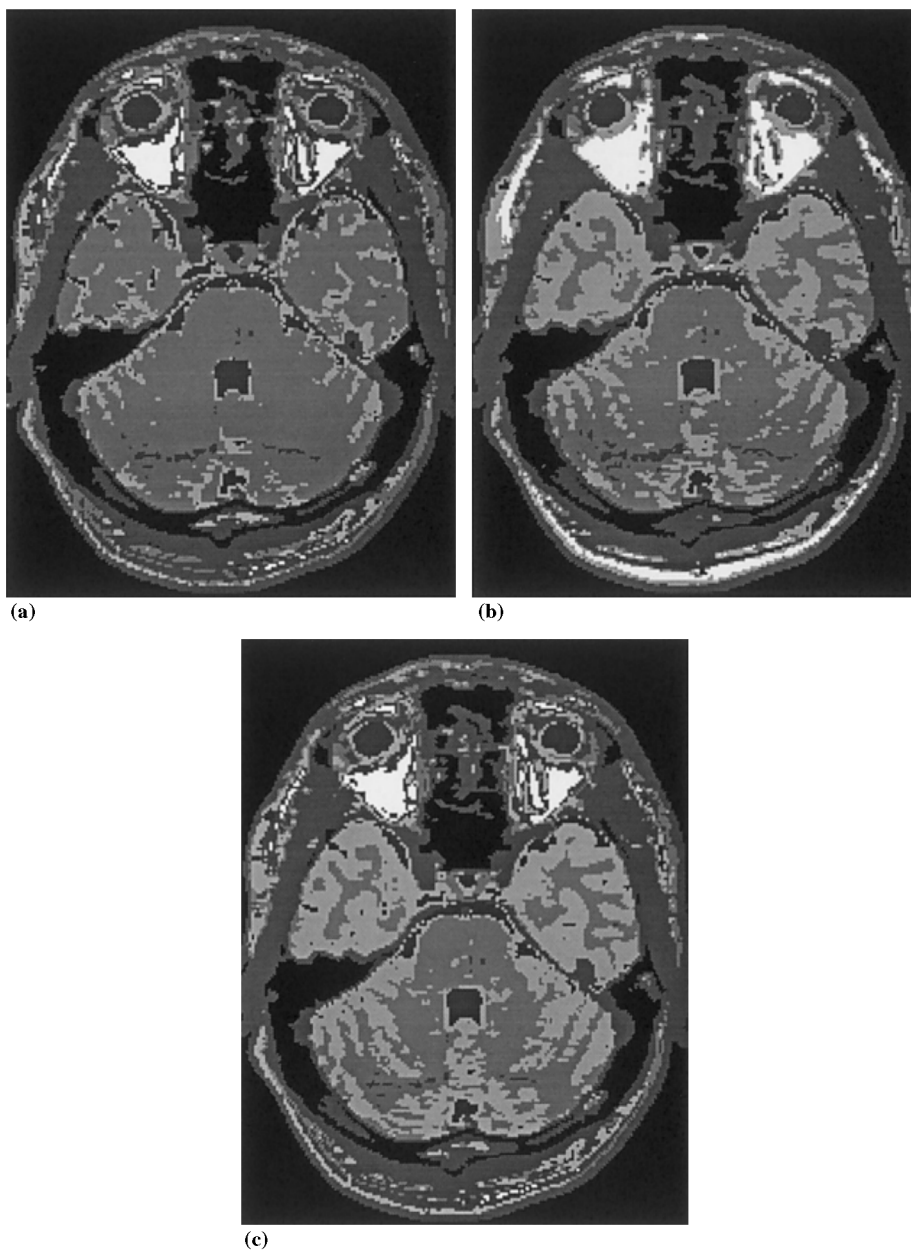


Fig. 4. Segmented images obtained by the CENN (a), the FCM (b), and the PNFCM (c) algorithms with five classes (normal patient).

On one hand, the CENN shows better performance with respect to the definition of the white and the grey matter, the separation between grey matter and tumor, and the homogeneity of the skull. On the other hand, FCM gives a better definition of edema. Both, however, give a noisy definition of the white matter.

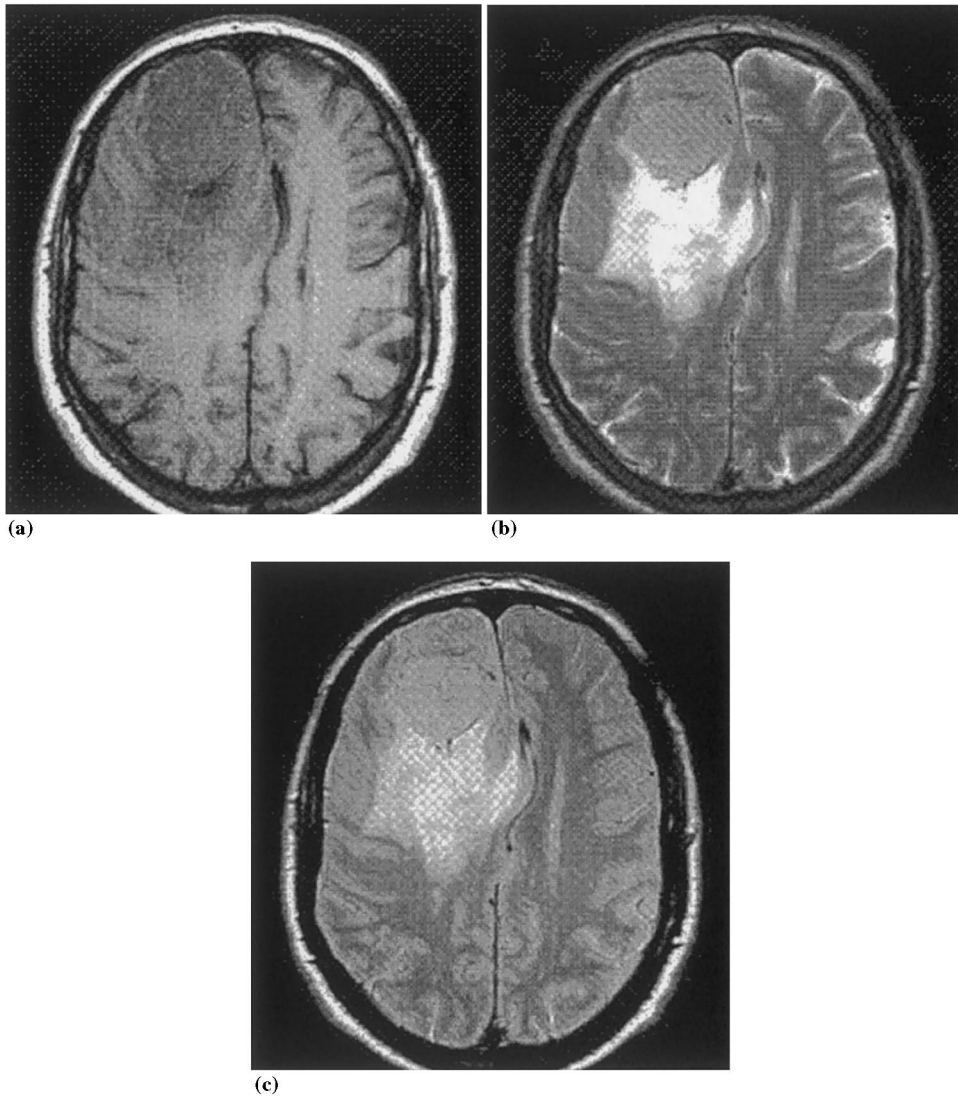


Fig. 5. T1-weighted (a), T2-weighted (b), and proton density (c) MRI images of a patient with meningioma in the right frontal lobe.

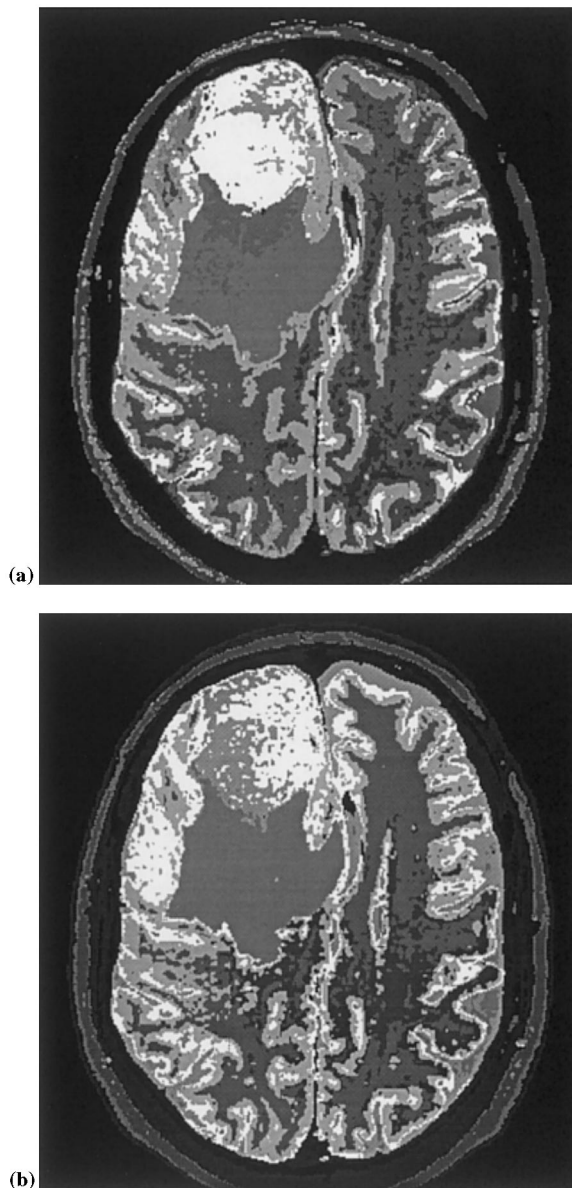


Fig. 6. Segmented images obtained by the CENN (a) and the FCM (b) algorithms with ten classes (patient with meningioma).

By applying the PNFCM algorithm, better results with only eight classes have been obtained (Fig. 7a), starting from those of the CENN bootstrap, improving the segmentation of tumor and edema, and moreover increasing the quality of the already good performances about grey matter and skull.

On the contrary, if a FCM segmentation with eight classes is performed, the results (Fig. 7b) show a poorly defined segmented image, where the separation between tumor and grey matter is lost as well as the distinction between edema and tumor.

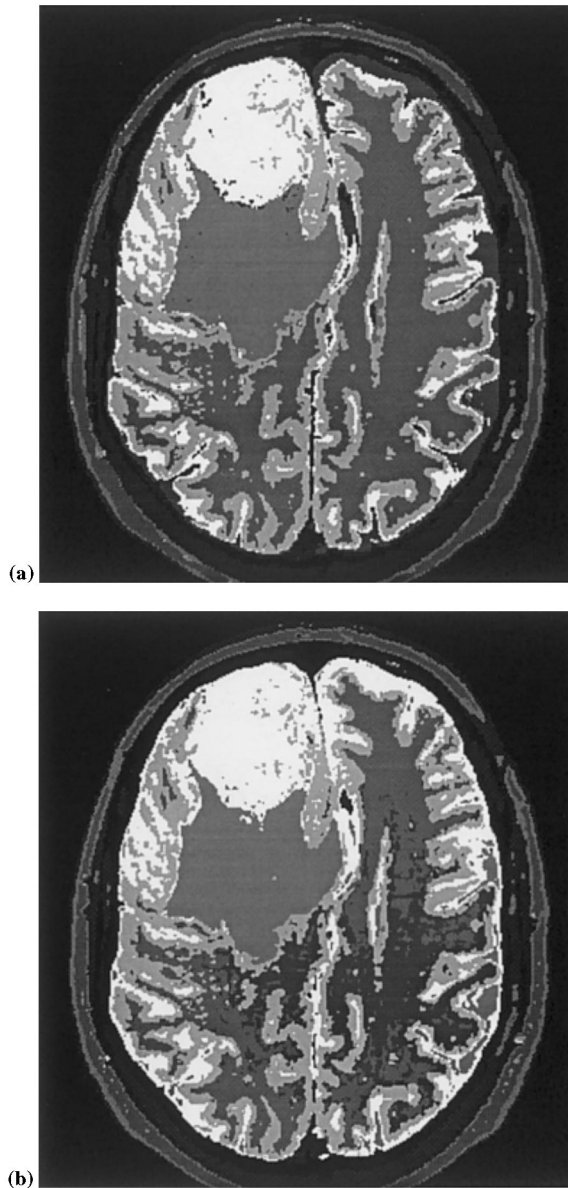


Fig. 7. Segmented images obtained by the PNFCM (a) and the FCM (b) algorithms with eight classes (patient with meningioma).

Table 1

Comparison scores for the normal patient using CENN, FCM, and PNFCM with five classes

	CENN (5)	FCM (5)	PNFCM (5)
White matter	0.43	0.74	0.91
Gray matter	0.36	0.61	0.83
Eyes/CSF	0.85	0.79	0.89
Skull	0.67	0.51	0.69

Table 2

Comparison scores for the patient with meningioma using CENN and FCM with ten classes and PNFCM and FCM with eight classes

	CENN (10)	FCM (10)	PNFCM (8)	FCM (8)
White matter	0.69	0.52	0.94	0.76
Gray matter	0.53	0.49	0.76	0.69
Edema	0.67	0.85	0.95	0.79
Tumor	0.58	0.45	0.74	0.58

In general the PNFCM algorithm can separate, in the feature space, classes with higher density and therefore with greater degree of typicality. At the same time it merged noisy classes in order to obtain a better homogeneity.

In comparison, FCM, initialized with a lower number of classes, did not obtain better results than FCM starting with more classes. The reason is that this algorithm tends to merge classes in the most significant regions of the feature space while even increasing the number of classes in very noisy regions.

In order to obtain a quantitative comparison between results from the different algorithms, we made, for both cases, an indirect comparison of the image, segmented by each algorithm, with a segmented image accepted by a pool of skilled clinicians, considered as a reference image. Comparison scores for each algorithm and for each class have been calculated by the equation

$$\sigma_{ij} \equiv \frac{A_{ij} \cap A_{refj}}{A_{ij} \cup A_{refj}}. \quad (18)$$

where A_{ij} represents the set of pixels belonging to the j th class found by the i th algorithm and A_{refj} represent the set of pixels belonging to the j th class in the reference segmented image. The results are shown in Table 1 for the normal case and in Table 2 for the meningioma case and confirm the qualitative evaluation.

7. Conclusions

For the diagnosis of pathologies through medical imaging, approaches based on clustering techniques [5,20,15,21,10] show higher robustness in discrimination of

regions than techniques based on edge detection [5], because of the low ratio signal/noise characterizing most of medical imaging data. Furthermore, fuzzy approaches to clustering turn out to be particularly interesting because, due to partial volume effects during acquisition, voxel values at the borders between volumes of interest correspond to mixtures of different anatomical tissues.

Computer-based image analysis systems for medical diagnosis should take this problem into account. Partial volume pixels can be considered as *fuzzy pixels*, with partial memberships to different kind of tissues. Unsupervised fuzzy clustering approach has proven to be well-suited to this type of problems normally competently handled by human diagnosticians.

The possibilistic approach to clustering [12,13], that treats the membership of a voxel to a tissue as a degree of *typicality*, is particularly useful. In the implementation, described in this paper, named the PNFCM algorithm, we combine a bootstrap based on the (CENN) [7] with the second version of the PCM-II [13] and a simple heuristic able to aggregate redundant clusters. The CENN avoids the estimation of the fuzzification parameter m and gives a robust estimation of the intracluster distance q_j . Moreover, the simple aggregating heuristic overcomes the problem of coincident clusters. As reported in Section 6, the PNFCM gives the best performance in the segmentation problem.

Since the main aim of computer based systems in medical imaging should be the support to the image analysis performed by physicians, each image processing function must be performed through high interactions with the user. The user has to maintain at each step the selection and the control of the analysis sequence. The right solution may be therefore a collection of integrated tools (black-boxes) performing specific processing on data, that physicians could tune and organize for specific diagnostic tasks.

In the design of the multimodal medical images segmentation system developed by our group [20] for supporting medical diagnosis, we took into account all these considerations. We used fuzzy clustering methods (including the PNFCM algorithm), and we developed a package for interaction with the user based on a X Window Motif interface. The resulting computer-based segmentation system reduces the diagnosis times and at the same time can out-perform, sometimes, the accuracy of non computer-supported diagnosis, especially when large sets of medical images, obtained with different modalities, are available.

Acknowledgements

This work was supported by PROGETTO SUD INFM and MURST. Images of the normal case are from Montreal Neurological Institute. Images of the meningioma case are from Department of Radiology University of Florida. We thank Nicolaos B. Karayiannis for fruitful interaction, and Marco Artuso for useful discussions.

References

- [1] Barni M, Capellini V, Mecocci A. Comments on ‘A possibilistic approach to clustering’. *IEEE Trans Fuzzy Syst* 1996;49:385–93.
- [2] Beni G, Liu X. A least biased fuzzy clustering method. *IEEE Trans Pattern Anal Mach Intell* 1994;16:954–60.
- [3] Bensaid AM, Hall LO, Clarke LP, Velthuizen RP. MRI segmentation using supervised and unsupervised methods. In: Nagel JH and Smith WM, editors. *Proceedings of the Thirteenth IEEE Engineering in Medicine and Biology Soc. Conference*. New York: IEEE, 1991:483–489.
- [4] Bezdek JC. *Pattern Recognition with Fuzzy Objective Function Algorithms*. New York: Plenum Press, 1981.
- [5] Bezdek JC, Hall LO, Clarke LP. Review of MR image segmentation techniques using pattern recognition. *Med Phys* 1993;20:1033–48.
- [6] Duda RO, Hart PE. *Pattern Classification and Scene Analysis*. New York: Wiley, 1973.
- [7] Firenze F, Morasso P. The capture effect model: a new approach to self-organized clustering. In: *Proceedings of the Sixth International Conference on Neural Networks and their Industrial and Cognitive Applications and Exhibition Catalog, NEURO-NIMES 93 Conference*. Nimes (France), 1993:45–54.
- [8] Gerig G, Martin J, Kikinis R, Kubler O, Shenton FA, Jolesz M. Unsupervised tissue type segmentation of 3D dual-echo MR head data. *Im Vis Comput* 1992;10:349–60.
- [9] Jaynes ET. Information theory and statistical mechanics. *Phys Rev* 1957;106:620–30.
- [10] Karayiannis NB. A methodology for construction of fuzzy algorithms for learning vector quantization. *IEEE Trans Neural Netw* 1997;8:505–18.
- [11] Kohonen T. *Self-Organizing Maps*. Berlin: Springer-Verlag, 1995.
- [12] Krishnapuram R, Keller JM. A possibilistic approach to clustering. *IEEE Trans Fuzzy Syst* 1993;1:98–110.
- [13] Krishnapuram R, Keller JM. The possibilistic c-means algorithm: insights and recommendations. *IEEE Trans Fuzzy Syst* 1996;4:385–93.
- [14] Maisey MN, et al. Synergistic imaging. *Eur J Nucl Med* 1992;19:1002–5.
- [15] Masulli F, Bogus P, Schenone A, Artuso M. Fuzzy clustering methods for the segmentation of multivariate images. In: Mares M, Mesia R, Novak V, Ramik J, Stupnanova A, editors. *Proceedings of the Seventh International Fuzzy Systems Association Word Congress IFSA '97, vol III*. Prague: Academia, 1997:123–128.
- [16] Masulli F, Bogus P, Schenone A, Artuso M. Application of MEP-based fuzzy clustering to the segmentation of multivariate medical images. In: Mancini D, Squillante M, Ventre A, editors. *New Trends in Fuzzy Systems, Proceedings of the International Joint Workshop on Current Issues on Fuzzy Technologies/Methods and Environments for Planning and Programming*. Singapore: World Scientific, 1998:266–277.
- [17] Pal NR, Pal K, Bezdek JC. A mixed c-means clustering model. In: *Proceedings of the International Conference on fuzzy Systems IEEE, FUZZ-IEEE '97*. Piscataway, NJ: IEEE, 1997:11–20.
- [18] Rose K, Gurewitz E, Fox G. A deterministic annealing approach to clustering. *Pattern Recognit Lett* 1990;11:589–94.
- [19] Rose K, Gurewitz E, Fox G. Constrained clustering as an optimization method. *IEEE Trans Pattern Anal Mach Intell* 1993;15:785–94.
- [20] Schenone A, Firenze F, Acquarone F, Gambaro M, Masulli F, Andreucci L. Segmentation of multivariate medical images via unsupervised clustering with adaptive resolution. *Comput Med Imaging Graph* 1996;20:119–29.
- [21] Schenone A, Masulli F, Artuso M. A neural bootstrap for the possibilistic c-means algorithm. In: Morabito FC, editor. *Advances in Intelligent Systems*. Amsterdam: IOS Press, 1997:359–66.